Available online at www.sciencedirect.com
SCIENCE DIRECT®
Journal of Sound and Vibration 270 (2004) 887–902
JOURNAL OF SOUND AND VIBRATION
www.elsevier.com/locate/jsvi

Crack identification in a rotor system: a model-based approach

A.S. Sekhar*

Technische Universität Darmstadt, Institut für Mechanik AG 2, Hochschulstrasse 1, D-64289 Darmstadt, Germany

Received 22 August 2002; accepted 3 February 2003

Abstract

The dynamics and diagnostics of cracked rotor have been gaining importance in recent years. In the present study a model-based method is proposed for the on-line identification of cracks in a rotor. The fault-induced change of the rotor system is taken into account by equivalent loads in the mathematical model. The equivalent loads are virtual forces and moments acting on the linear undamaged system to generate a dynamic behaviour identical to the measured one of the damaged system. The rotor has been modelled using finite element method, while the crack is considered through local flexibility change. The crack has been identified for its depth and location on the shaft. The nature and symptoms of the fault, that is crack, are ascertained using the fast fourier transform.

1. Introduction

An important rotor fault, which can lead to catastrophic failure if undetected, is fatigue cracks in the shaft. Vibration behaviour of cracked structures, in particular cracked rotors has received considerable attention in the last three decades [1–3]. The problem of damage and crack identification in structural components has acquired an important role in recent years.

The increasing concern over early crack detection or rotor failures due to the presence of crack has accelerated the development of non-destructive techniques based on changes of the modal parameters of the system [4]. As summarized by Hamidi et al. [4], several publications have proposed the use of a number of techniques such as the use of natural frequencies, mode shapes and frequency response functions for damage detection.

It has been seen that new model-based fault diagnosis techniques are being developed rapidly in order to meet the demand for increasingly intelligent condition monitoring systems for the

*Corresponding author. Department of Mechanical Engineering, Indian Institute of Technology, Kharagpur 721 302, India. Tel.: +91-3222-282976; fax: +91-3222-255303.
E-mail address: sekhar@mech.iitkgp.ernet.in (A.S. Sekhar).

0022-460X/$ - see front matter © 2003 Elsevier Ltd. All rights reserved.
doi:10.1016/S0022-460X(03)00637-0

maintenance of modern industrial process. Seibold and Weinert [5] investigated detection techniques based on extended Kalman filters to detect the position and depth of crack whereby each filter represents a difference damage scenario. Recently, Markert et al. [6–8] proposed a model based method which allows the on-line identification of malfunctions in rotor systems. They presented the models in which equivalent loads due to the faults such as rubbing and unbalance as virtual forces and moments acting on the linear undamaged system model to generate a dynamic behaviour are identical to the measured one of the damaged system. The identification is then performed by least-squares fitting in the time domain. Edwards et al. [9] employed a model-based identification in the frequency domain to identify an unbalance on a test-rig. A more comprehensive approach to identify different types of faults has been reported in Ref. [10].

For diagnosing the state of a machine usually signal-based monitoring systems are used as good tools, although they do not fully utilize the information contained within the vibration data. These approaches to machinery diagnostics are generic rather than machine specific and the interpretation of the data is based on qualitative rather than quantitative information. Contrary to signal-based monitoring systems, model-based diagnostics systems developed in recent years [11,12] utilize all information contained in the continuously recorded vibration signals. These methods work either in the time or in the frequency domain depending on the malfunction type and the operating state for which the vibration data are available. Also it can be used together with or alternatively to conventional signal based monitoring systems.

In the present study the model-based method is applied to identify the crack in the rotor at a steady speed. The presence of crack in time domain has been identified through some equivalent loads acting at the nodes of cracked finite element. Bach and Markert [6] have presented a model-based technique for the crack identification, in which, from a few measured quantities the full system state is reconstructed by an observer during an iterative procedure. However, unlike that previous case the full state is estimated through modal expansion in the present study and systematic crack identification is done with model based approach together with FFT.

2. Identification method

In the present study model-based identification method [7,8] is used, which is based on the idea that system faults can be represented by virtual loads ΔF that act on the linear undamaged system model. Equivalent loads are fictitious forces and moments which generate the same dynamic behaviour as the real non-linear damaged system does. This method enables to maintain linear, so that fast analysis can be carried out to identify faults while the machine is still running.

2.1. Mathematical description

The vibrations represented by the vector $\mathbf{r}_o(t)$ with N degrees of freedom of the undamaged rotor system due to the operating load $\mathbf{F}_o(t)$ during normal operation are described by the linear equation of motion:

$$\mathbf{M}_o\ddot{\mathbf{r}}_o(t) + \mathbf{D}_o\dot{\mathbf{r}}_o(t) + \mathbf{K}_o\mathbf{r}_o(t) = \mathbf{F}_o(t), \tag{1}$$

where $\mathbf{M}_o$, $\mathbf{D}_o$, $\mathbf{K}_o$ are mass, damping and stiffness matrices of any complex rotor system, which can include the effects of bearings, foundation, gyroscopic forces, etc.

The occurrence of a fault changes the dynamic behaviour of the system, the extent of the change depends on the vector $\boldsymbol{\beta}$, which describes the fault parameters like type, magnitude, location, etc. of the fault. The fault-induced change in the vibrational behaviour is represented by the additional loads acting on the undamaged system.

$$\mathbf{M}_o\ddot{\mathbf{r}}(t) + \mathbf{D}_o\dot{\mathbf{r}}(t) + \mathbf{K}_o\mathbf{r}(t) = \mathbf{F}_o(t) + \Delta\mathbf{F}(\boldsymbol{\beta}, t). \tag{2}$$

The residual vibrations induced represent the difference of the previously measured normal vibrations of the undamaged system from vibrations of the currently measured damaged system:

$$\Delta\mathbf{r}(t) = \mathbf{r}(t) - \mathbf{r}_o(t), \quad \Delta\dot{\mathbf{r}}(t) = \dot{\mathbf{r}}(t) - \dot{\mathbf{r}}_o(t), \quad \Delta\ddot{\mathbf{r}}(t) = \ddot{\mathbf{r}}(t) - \ddot{\mathbf{r}}_o(t). \tag{3}$$

Subtraction of the equations of motion for the undamaged, Eq. (1), from that of the damaged, Eq. (2), and using Eq. (3), yields the equation of motion for the residual vibration as given by

$$\mathbf{M}_o\Delta\ddot{\mathbf{r}}(t) + \mathbf{D}_o\Delta\dot{\mathbf{r}}(t) + \mathbf{K}_o\Delta\mathbf{r}(t) = \Delta\mathbf{F}(\boldsymbol{\beta}, t). \tag{4}$$

The system matrices remain unchanged, the rotor model stays linear. Only the equivalent loads induce the change in the dynamic behaviour of the undamaged linear rotor model. To identify the fault parameters, the difference of the theoretical fault model and the measured equivalent loads will be minimized by a least-squares fitting algorithm.

For calculating the fault-induced residual vibrations, measured vibration data for both the undamaged and damaged rotor system have to be available for the same operating and measurement conditions. For example, differences in the rotor speeds, phase and the sampling times have to be taken into account. Because directly matching data are usually not available, some signal processing has to be done to achieve the same conditions. Different rotor speeds, for instance, are compensated by adjusting the time scale of the recorded normal vibrations to the time scale of the currently measured vibrations. Differences in the sampling frequencies can be eliminated by interpolating the recorded normal vibrations to the sampling times of the current measurement. The phase shifts are avoided by recording a trigger signal [7,8].

2.2. Modal expansion

For calculating the equivalent loads from the mathematical model of the rotor system by Eq. (4), measured residual vibrations must be available in all the degrees of freedom (DOF) of the model. Since the vibrations are measured only at a few DOF in practice, the vibrations at non-measured DOF must be estimated using the measured vibrations. Therefore, the residual vibrations need to be reconstructed via modal expansion from the directly measured vibrations such as $\Delta\tilde{\mathbf{r}}_M(t)$, at the measuring positions. This technique is based on the approximation of the residual vibration by a linear combination of only a few eigenvectors. Simultaneously, a set of equivalent loads representing the malfunctions is calculated from the measured vibration signals using the mathematical model of the undamaged rotor system.

By comparing the equivalent loads reconstructed from the current measurements to the pre-calculated equivalent loads resulting from fault models, the type, amount and location of the current fault can be estimated. The identification method is based on least-squares fitting

algorithms in the time domain. The quality of the fit is used to find the probability that the identified fault is present.

As explained before, the residual vibrations $\Delta\tilde{\mathbf{r}}_M(t)$ are available only for a few DOF of the model. The number M of the measurement locations is much smaller than the number N, the DOF of the model. The data of the non-measurable DOF have to be estimated from the measured signals. The measurable part $\Delta\tilde{\mathbf{r}}_M(t)$ of the residual vector is related to the full residual vector $\Delta\tilde{\mathbf{r}}(t)$ by the measurement matrix $\mathbf{C}$,

$$\Delta\tilde{\mathbf{r}}_M(t) = \mathbf{C}\Delta\tilde{\mathbf{r}}(t). \tag{5}$$

The full residual vector can be approximated by a set of mode shapes $\widehat{\mathbf{r}}_k$ which are put together in the reduced modal matrix:

$$\widehat{\boldsymbol{\phi}} = [\widehat{\mathbf{r}}_1, \widehat{\mathbf{r}}_2, \ldots, \widehat{\mathbf{r}}_k]. \tag{6}$$

Logically, the number K of mode shapes used may not exceed the number M of independently measured vibration signals contained in $\tilde{\mathbf{r}}_M(t)$, $K \leqslant M$. The vector of modal co-ordinates $\Delta\mathbf{q}(t)$ is estimated by combining the measurement equation (5) with modal representation

$$\Delta\tilde{\mathbf{r}}(t) = \widehat{\boldsymbol{\phi}}\,\Delta\mathbf{q}(t) \tag{7}$$

of the full residual vector and minimising the equation error by the least-squares method. Eventually, the full residual vector at all DOF is estimated by

$$\Delta\tilde{\mathbf{r}}(t) = \{\widehat{\boldsymbol{\phi}}[(\mathbf{C}\,\widehat{\boldsymbol{\phi}})^{\mathrm{T}}(\mathbf{C}\,\widehat{\boldsymbol{\phi}})]^{-1}\ [\mathbf{C}\,\widehat{\boldsymbol{\phi}}]^{\mathrm{T}}\}\Delta\tilde{\mathbf{r}}_M(t) = \mathbf{Q}\Delta\tilde{\mathbf{r}}_M(t), \tag{8}$$

where the constant matrix $\mathbf{Q}$ can be calculated in advance.

2.3. Equivalent loads

The equivalent load $\Delta\tilde{\mathbf{F}}(t)$ characterizing the unknown fault is calculated by substituting the residual vibrations of the full vibrational state into Eq. (4), together with Eq. (8), yielding

$$\Delta\tilde{\mathbf{F}}(t) = \mathbf{M}_{\mathrm{o}}\mathbf{Q}\Delta\ddot{\tilde{\mathbf{r}}}_M(t) + \mathbf{D}_{\mathrm{o}}\mathbf{Q}\Delta\dot{\tilde{\mathbf{r}}}_M(t) + \mathbf{K}_{\mathrm{o}}\mathbf{Q}\Delta\tilde{\mathbf{r}}_M(t). \tag{9}$$

Only simple matrix multiplications and additions have to be carried out, for estimating the equivalent loads from the measured vibration signals. Thus, it is very suitable for on-line identification of crack or any other fault.

2.4. Fault models

For the model-based fault identification method, each fault has to be represented by a mathematical model describing the relation between the fault parameters $\boldsymbol{\beta}$ and the equivalent force $\Delta\tilde{\mathbf{F}}(t)$. Hence, $\Delta\mathbf{F}(\boldsymbol{\beta}, t)$ is a mathematical expression for the time history of the forces acting on the individual DOF of the model. The fault vector $\boldsymbol{\beta}$ in this case contains the crack depth and location. A detailed explanation of the crack, the fault considered in this paper is given in a separate section. The basic idea to model a transverse crack in a shaft is to consider the change of the cracked element's stiffness. The changed stiffness of the cracked element is multiplied with the

displacement vector $\mathbf{r}(t)$ which yields in the equivalent force,

$$\Delta\mathbf{F}_{cr}(\boldsymbol{\beta}, t) = \Delta\mathbf{K}\mathbf{r}(t). \tag{10}$$

2.5. Least-squares fitting in the time domain

For identifying the fault parameters, the equivalent loads from measured vibrations and those from the mathematical model should be compared. If there were no noise and no errors due to modal expansion, the equivalent loads from measured data would match exactly to loads of a certain fault model. Since the measured signals and their processing is always associated with some noise and inevitable errors, the best fit between the two loads patterns is sought by adjusting the fault parameters. The least-squares algorithm is used in time domain to achieve the best curve fitting. The objective function to be minimized for the measured equivalent forces $\Delta\tilde{\mathbf{F}}(t)$ and the theoretical ones $\Delta\mathbf{F}_i(\boldsymbol{\beta}_i, t)$, as

$$\int \left| \sum_i \Delta\mathbf{F}_i(\boldsymbol{\beta}_i, t) - \Delta\tilde{\mathbf{F}}(t) \right|^2 \mathrm{d}t = Min. \tag{11}$$

The algorithm iterates for the values of fault parameters $\boldsymbol{\beta}_i$ for all suspected faults taken into account. This eventually leads to identification of the fault type, its position and the extent.

2.6. Probability measures

The quality of fit achieved can be used to estimate the probability of the different identified faults. Two probability measures based on correlation functions have been developed and successfully tested in Ref. [8]. These are also used here.

The first probability measure p_1, called coherence, is the normalized correlation of the identified equivalent forces $\Delta\mathbf{F}_i(\boldsymbol{\beta}_i, t)$ of a particular fault with the measured equivalent forces $\Delta\tilde{\mathbf{F}}(t)$ for lag $\tau = 0$,

$$p_1 = \phi_{\Delta F_i, \Delta\tilde{F}}(0) / \sqrt{\phi_{\Delta F_i, \Delta F_i}(0)\phi_{\Delta\tilde{F}(t), \Delta\tilde{F}}(0)}. \tag{12}$$

Due to the normalization by the auto-correlation functions of $\Delta\mathbf{F}_i(\boldsymbol{\beta}_i, t)$ and $\Delta\tilde{\mathbf{F}}(t)$, the coherence takes values between $-1 \leqslant p_1 \leqslant 1$, where $p_1 = 1$ means that $\Delta\mathbf{F}_i(\boldsymbol{\beta}_i, t)$ matches $\Delta\tilde{\mathbf{F}}(t)$ perfectly.

The other probability measure p_2, called the intensity, measures the contribution of the particular fault to the measured total equivalent forces $\Delta\mathbf{F}_{ident} = \sum\Delta\mathbf{F}_i$,

$$p_2 = \phi_{\Delta F_i, \Delta F_i} / \phi_{\Delta F_{ident}, \Delta F_{ident}}(0). \tag{13}$$

The intensity measures takes values in the interval $0 \leqslant p_2 \leqslant 1$, where $p_2 = 1$ signifies that the identified fault is the only one present in the rotor system. It was reported in Refs. [7,8], that both measures p_1 and p_2 should be used simultaneously to evaluate the probability of a fault. Suitable threshold values are $p_1 \geqslant 10\%$ and $p_2 \geqslant 20\%$ indicating that specific fault is present in the rotor system [8].

The whole process of identification is shown in Fig. 1. The measured vibration signals $\tilde{\mathbf{r}}_M(t)$ are the input and the fault parameters $\boldsymbol{\beta}_i$ for each fault are the output.

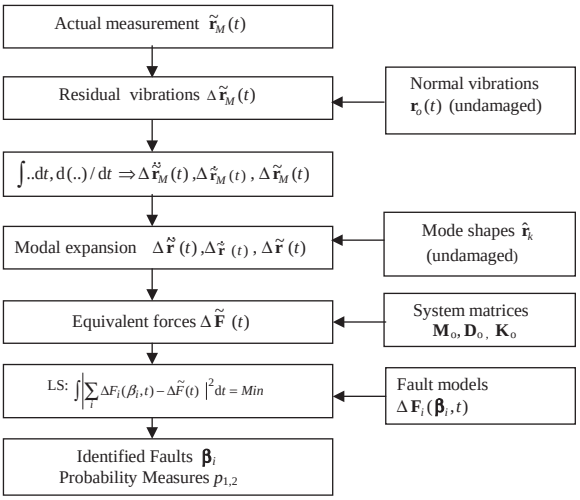

Fig. 1. Flow chart of the fault identification method.

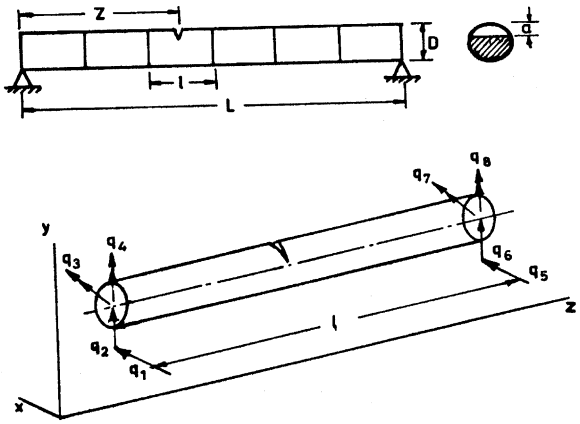

Fig. 2. Simply supported shaft with a cracked element.

3. System equation of motion

The rotor-bearing system is discretized into finite beam elements [13] as shown in Fig. 2, together with details of shaft element. Even though the figure is shown with crack, all the configuration and details are also valid for uncracked rotor. The equation of motion of the complete rotor system in a fixed co-ordinate system can be written as

$$[\mathbf{M}]\{\ddot{\mathbf{q}}\} + [\mathbf{D}]\{\dot{\mathbf{q}}\} + [\mathbf{K}]\{\mathbf{q}\} = \{\mathbf{F}\}, \tag{14}$$

where the mass matrix [**M**] includes the rotary and translational mass matrices of the shaft, mass and diametral moments of the rigid disc. The matrix [**D**] includes the gyroscopic moments, and

damping. The stiffness matrix [**K**] considers the stiffness of the shaft elements and the bearing stiffness. Cracked element stiffness can be included easily, for the cracked rotor analysis. The excitation matrix {**F**} in Eq. (14) consists of the unbalance forces due to disc having mass m, eccentricity e and the weight of the disc.

4. Crack modelling

The transverse breathing crack has been considered in the present study. There are several ways to model the crack as mentioned in Ref. [3]. In the present study, the flexibility matrices of the cracked section as given in Ref. [14] are utilized for crack modelling. The flexibility coefficients for an element without crack by neglecting shearing action are given by

$$\mathbf{C}_0 = \begin{bmatrix} l^3/3EI & & SYM & \\ 0 & l^3/3EI & & \\ 0 & -l^2/2EI & l/EI & \\ l^2/2EI & 0 & 0 & l/EI \end{bmatrix},$$

where EI is the bending stiffness and l is the element length. During the shaft's rotation, the crack opens and closes (the breathing action of the crack) depending on the rotor deflection [15]. For the large class of machines, the static deflection is much greater than the rotor vibration. With this assumption the crack is closed when $\phi = 0$ and it is fully open when $\phi = \pi$ (see Fig. 3). The transverse surface crack on the shaft element introduces considerable local flexibility due to strain energy concentration in the vicinity of the crack tip under load. The additional strain energy due to the crack results in a local flexibility matrix $\mathbf{C}_c$ which will be $\mathbf{C}_{op}$ and $\mathbf{C}_{HC}$ for a fully open crack

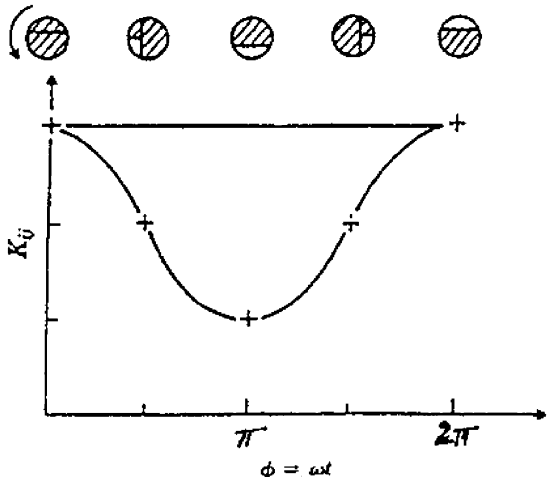

Fig. 3. Breathing crack model.

and half-open, half-closed conditions, respectively:

$$\mathbf{C}_{op} = \frac{1}{F_0}\begin{bmatrix} \bar{C}_{11}R & & SYM & \\ 0 & \bar{C}_{22}R & & \\ 0 & 0 & \bar{C}_{33}/R & \\ 0 & 0 & \bar{C}_{43}/R & \bar{C}_{44}/R \end{bmatrix},$$

$$\boldsymbol{C}_{HC} = \frac{1}{2F_0}\begin{bmatrix} \bar{C}_{22}R & & SYM & \\ 0 & \bar{C}_{11}R & & \\ 0 & 0 & \bar{C}_{44}/R & \\ 0 & 0 & \bar{C}_{34}/R & \bar{C}_{33}/R \end{bmatrix},$$

where $F_0 = \pi ER^2/(1-\upsilon^2)$, $R = D/2$ and $\upsilon = 0.3$. The dimensionless compliance coefficients, $\bar{c}_{ij}$, are functions of non-dimensional crack depth, $\bar{\alpha}(\alpha/\mathrm{D})$, where α is the crack depth in shaft diameter D (see Fig. 2). These compliance coefficients are computed from the derivations discussed in Ref. [14]. The total flexibility matrix for the cracked section is given as [15]

$$[\mathbf{C}] = [\mathbf{C}_0] + [\mathbf{C}_c]. \tag{15}$$

As explained before, $\mathbf{C}_c$ will be $\mathbf{C}_{op}$ or $\mathbf{C}_{HC}$ depends on the breathing position of crack (see Fig. 3).

From the equilibrium condition (see Fig. 2)

$$(q_1, q_2, \ldots, q_8)^{\mathrm{T}} = [T](q_5, \ldots, q_8)^{\mathrm{T}}, \tag{16}$$

where the transformation

$$T = \begin{bmatrix} -1 & 0 & 0 & -l & 1 & 0 & 0 & 0 \\ 0 & -1 & l & 0 & 0 & 1 & 0 & 0 \\ 0 & 0 & -1 & 0 & 0 & 0 & 1 & 0 \\ 0 & 0 & 0 & -1 & 0 & 0 & 0 & 1 \end{bmatrix}^{\mathrm{T}}.$$

4.1. Stiffness matrix

The stiffness matrix of the cracked element is written as [15]

$$[\mathbf{K}_c] = [\mathbf{T}][\mathbf{C}]^{-1}[\mathbf{T}]^{\mathrm{T}}. \tag{17}$$

When the shaft is cracked, during the rotation the stiffness varies with time, or with angle. The variation may be expressed by a truncated cosine series

$$[\mathbf{K}] = [\mathbf{K}_0] + [\mathbf{K}_1]\cos\omega t + [\mathbf{K}_2]\cos 2\omega t + [\mathbf{K}_3]\cos 3\omega t + [\mathbf{K}_4]\cos 4\omega t, \tag{17'}$$

where $[\mathbf{K}_\eta]$, $\eta = 0, 1, \ldots, 4$, are fitting coefficient matrices, determined from the known behaviour of the stiffness matrix at certain angular locations [15]. These are obtained from the compliance matrices $\mathbf{C}_0$, $\mathbf{C}_{op}$ and $\mathbf{C}_{HC}$ together with Eq. (17).

5. Results and discussion

A rotor system with two flexible bearings and two rigid disks as shown in Fig. 4, has been considered in the present analysis. The data for the rotor system are given in Table 1. The analysis has been carried out using FEM for flexural vibrations. The eigenvalues are given in Table 2,

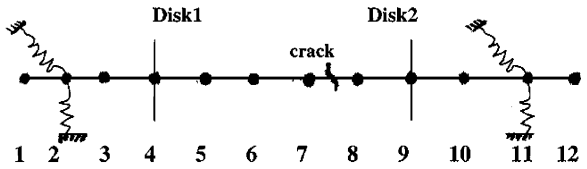

Fig. 4. Typical rotor-bearing system considered.

Table 1
Rotor-bearing data

Length of the rotor, L		0.780 m
Shaft		
Diameter, D		0.02 m
Density		7850 kg/m^3
Modulus of elasticity		2.1×10^{11} N/m^2
Discs		
Masses: m_1, m_2		6.45, 4.27 kg
Unbalance eccentricity		0.01 mm
Crack		
Location		6 and 7 element
Depth, α		1.4, 2 and 4 mm
Non-dimensional depth, $\bar{\alpha}(\alpha/D)$		0.07, 0.1 and 0.2
Bearing stiffness (N/m)		
Left bearing stiffness	in horizontal direction	0.105×10^6
	in vertical direction	0.150×10^6
Right bearing stiffness	in horizontal direction	1.06×10^6
	in vertical direction	1.02×10^6
Speed of the rotor, ω		4420 rpm (73.7 Hz) and 7800 rpm (130 Hz)

Table 2
Eigenfrequencies of rotor system

Mode no.	Eigenfrequencies (Hz)
1	16.85 (H)
2	28.16 (V)
3	30.38 (H)
4	70.24 (V)
5	71.63 (H)
6	124.76 (V)

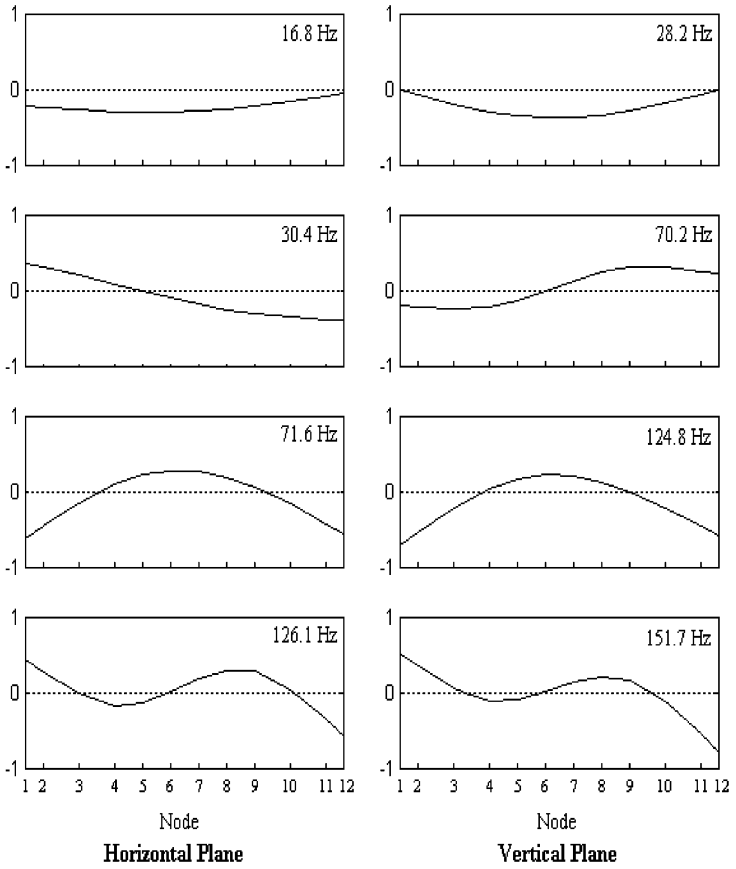

Fig. 5. Mode shapes of rotor system.

while the mode shapes are shown in Fig. 5. The analysis has been carried out at a steady speed of 4420 rpm (73.7 Hz). A crack at the mid of the rotor and in the center of the element 7 (see Fig. 4) is considered for the study. Houbolt time marching technique is used due to better convergence of results [15], to model the system in time domain with a time step of 0.001 s.

In the present study, in the beginning, the vibrations are considered in all the 48 degrees of freedom (DOF) of the model, and this is considered as a reference case. However, normally the vibrations are measured only with a few sensors or transducers. Hence, the measured vibration data are available only for a few DOF. Thus the study is done considering less than 48 DOF, such as with 24, 20, ...4 DOF. For such a few DOF, the vibration data at all the DOF of the rotor are estimated using the modal expansion as explained in Section 2.2. The identification algorithm is searched for crack.

The typical results with crack depths 1.4, 2 and 4 mm are given in the Tables 3–5. In all these tables and in subsequent figures showing the results, one point is to be noted. The measured data available at certain DOF means, as explained previously that the vibration data are available only at such DOF. In this study no experimental data are available, but it is simulated using modal expansion for few DOF. In the absence of experimental validations, the simulation results are

Table 3
Results of crack identification (crack of depth 1.4 mm in element no. 7)

Case.no	Measured data available at	Estimated crack location (element no.)	Estimated crack depth (α in mm)	Probability measures in %	
				Coherence	Intensity
1	Sensors at 48 DOF (Reference case)	7	1.40	100.0	25.0
2	Noise signals	7	1.398	99.89	24.98
3	Modelling error	7	1.370	100.0	25.0
4	Calibration error	7	1.40	99.99	25.0
5	24 DOF	7	1.12	99.99	24.41
6	20 DOF	7	0.96	99.99	19.60
7	16 DOF	7	0.56	99.99	19.13
8	8 DOF	7	0.32	99.98	25.0
9	4 DOF	7	0.30	99.98	25.0

Table 4
Results of crack identification (crack of depth 2 mm in element no. 7)

S.no	Measured data available at	Estimated crack location (element no.)	Estimated crack depth (α in mm)	Probability measures in %	
				Coherence	Intensity
1	48 DOF (Reference case)	7	2.0	100	25.0
2	24 DOF	7	1.6	99.99	24.40
3	20 DOF	7	1.4	99.93	19.40
4	16 DOF	7	0.80	99.90	20.0
5	8 DOF	7	0.40	99.99	25
6	4 DOF	7	0.32	99.90	25

Table 5
Results of crack identification (crack of depth 4 mm in element no.7)

S.no	Measured data available at	Estimated crack location (element no.)	Estimated crack depth (α in mm)	Probability measures in %	
				Coherence	Intensity
1	48 DOF (Reference case)	7	4.0	100	25.0
2	24 DOF	7	3.1	99.93	24.38
3	20 DOF	7	2.6	99.93	18.39
4	8 DOF	7	1.3	99.97	25.0
5	4 DOF	7	1.3	99.90	25.0

presented with several effects such as noise, etc. contaminating the simulations. The simulations were done with the effects of measurement noise, modelling error and calibration error for one crack depth and are given in Table 3. The results showed their effects to be very low (hence, these

effects are not considered in Tables 4 and 5) thus showing the effectiveness of the identification method/approach. These are discussed in the following paragraphs (refer to Table 3).

Case 1: The time histories of displacements, velocities and accelerations were exactly measured at all the 48 DOF of the rotor system, so modal expansion was not necessary. The crack depth and location were identified exactly. This case was considered as reference case.

Case 2: In this case all the measuring signals were falsified by band-limited noise. The standard deviation of the disturbances was about 2% of the amplitude of the correct signal. The crack has been identified exactly in element 7 with negligible error in estimating the depth.

Case 3: In this case 5% modelling error has been introduced in both stiffness and mass matrix. In this case also, the crack has been identified exactly in element 7 with negligible error in estimating the depth.

Case 4 : In this case calibration errors of 10% in the sensors at both bearings (also at disks separately) were simulated. The crack depth and location were identified exactly.

Cases 5–9 : Normally, the vibrations are measured only with a few sensors or transducers. Hence, the measured vibration data are available only for a few DOF. Thus the study is done considering less than 48 DOF, such as with $24, 20, \ldots 4$ DOF in cases 5–9. The modal expansion technique has been used in these cases.

The results show that even for the small crack (1.4 mm or $\alpha = 0.07$) and with fewer measured data (less DOF such as 4, 8), the location of crack has been identified effectively. The results show that with decrease in measured vibration data (less DOF) the error in estimating the depth has increased. This is expected as the full vibration data of unmeasured locations using the mode shape of an undamaged rotor system cannot be accurately estimated from fewer data points. However, the location has been identified successfully.

One should not get misled by the depth it has been estimated on-line and proceed to continue running the rotor. As per the results which can be noticed from Tables 3–5, the error in estimating the depth of crack is on an average of the order of 75% when using a few sensors or a lesser number of DOF. Thus, the crack depth should be estimated by considering this error, if to determine when the machine must be removed from service. However, better expansion techniques or refined modal expansion methods should be incorporated to get better results and to finally implement this scheme in practice.

The crack identification process using a model-based method algorithm with the residual vibrations, estimated the equivalent loads for the reference case (48 DOF) and is shown in Fig. 6.

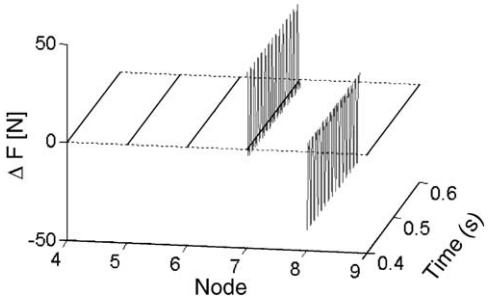

Fig. 6. Reference case (48 DOF): estimated equivalent loads, for crack of depth 4 mm in element 7.

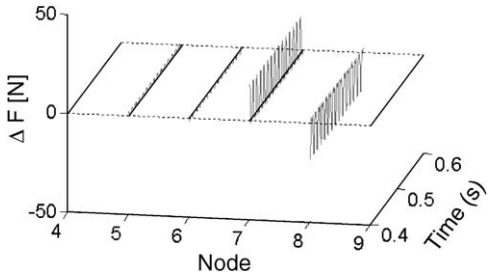

Fig. 7. Estimated equivalent loads (24 DOF), for crack of depth 4 mm in element 7.

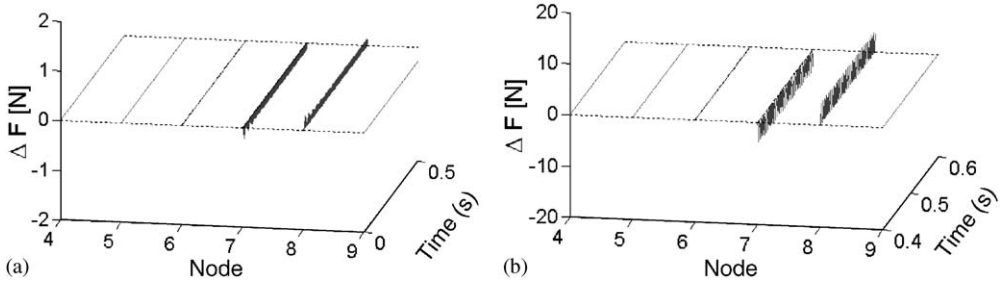

Fig. 8. (a) Estimated equivalent loads (4 DOF), crack of depth 1.4 mm in element 7. (b) Estimated equivalent loads (4 DOF), crack of depth 4 mm in element 7.

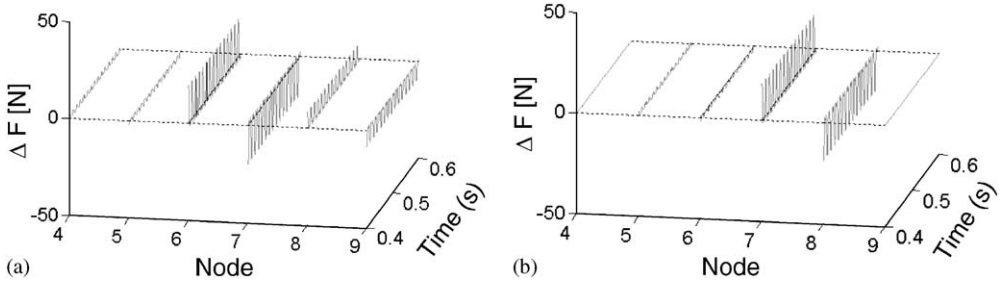

Fig. 9. Estimated equivalent loads (24 DOF) for different crack locations, Crack depth 4 mm (a) crack in 6th element, (b) crack in 7th element.

From this figure, it is clear that the equivalent forces are observed only at nodes 7 and 8 which are the nodes of the cracked element. Hence, this method identified the crack at the exact location and also estimated the depth correctly (20% of the shaft diameter = 4 mm, see Table 5). Further, the crack identification results with fewer measured data (less DOF) are shown in Figs. 7 and 8. In all the cases, including the case of 4 DOF (see Figs. 8a and b), the equivalent forces are observed to dominate at the nodes (Figs. 7 and 8) of the cracked element no. 7. That means the crack location has been identified successfully.

The location of the crack has been changed from seventh to sixth. Then also the crack has been identified at the correct location. The details are shown in Figs. 9a and b. But, for the estimation

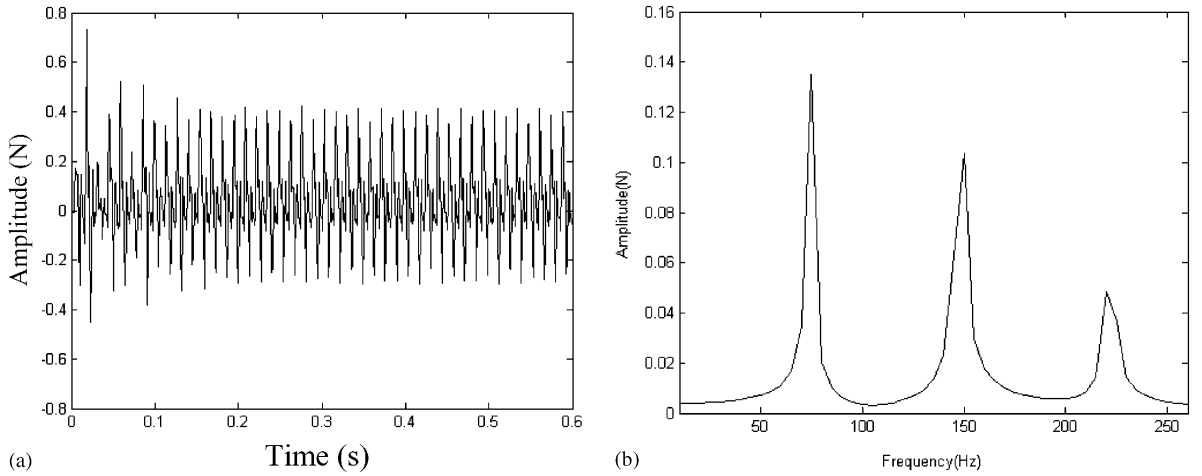

Fig. 10. (a) Estimated equivalent load versus time for crack of depth 2 mm in element 7 (8 DOF) (b) Estimated equivalent load versus frequency for crack of depth 2 mm (FFT of Fig. 10a).

of crack depth, the error has increased with the few measured data, as explained before. Further, the symptoms of the present fault are found using the FFT of Fig. 10a, the time response of equivalent force. Fig. 10b shows the FFT of the estimated equivalent force. It can be observed clearly from Fig. 10b, the $2\times$, $3\times$ harmonic components (first peak corresponds to 73.7 Hz, the running speed). These harmonics are the characteristics of crack.

The simulation has been repeated for a different speed of the rotor, 7800 r.p.m. (130 Hz), the results of which are shown in Fig. 11. The results show that the crack has been identified successfully and from Fig. 11c, the FFT shows the harmonic components which are the characteristics of crack. If the experimental results are available one can easily use them as measured data and apply the modal expansion to identify the crack effectively.

The model-based identification technique with modal expansion has been successfully demonstrated for crack location. For the better estimation of crack depth, one can refine the modal expansion, considering some weighting functions or some suitable curve fitting functions, etc., together with the mode shapes.

6. Conclusion

A complex rotor-bearing system has been modelled using FEM. The model-based identification technique with modal expansion has been successfully demonstrated for different crack locations and depths at different rotor speeds. The nature and symptoms of the fault, that is crack, are ascertained using the FFT. The effectiveness of the identification process depends to a good extent on the number of measured locations (DOF). However, this is only for estimating the crack depth. The present approach allows for effective on-line crack identification effectively.

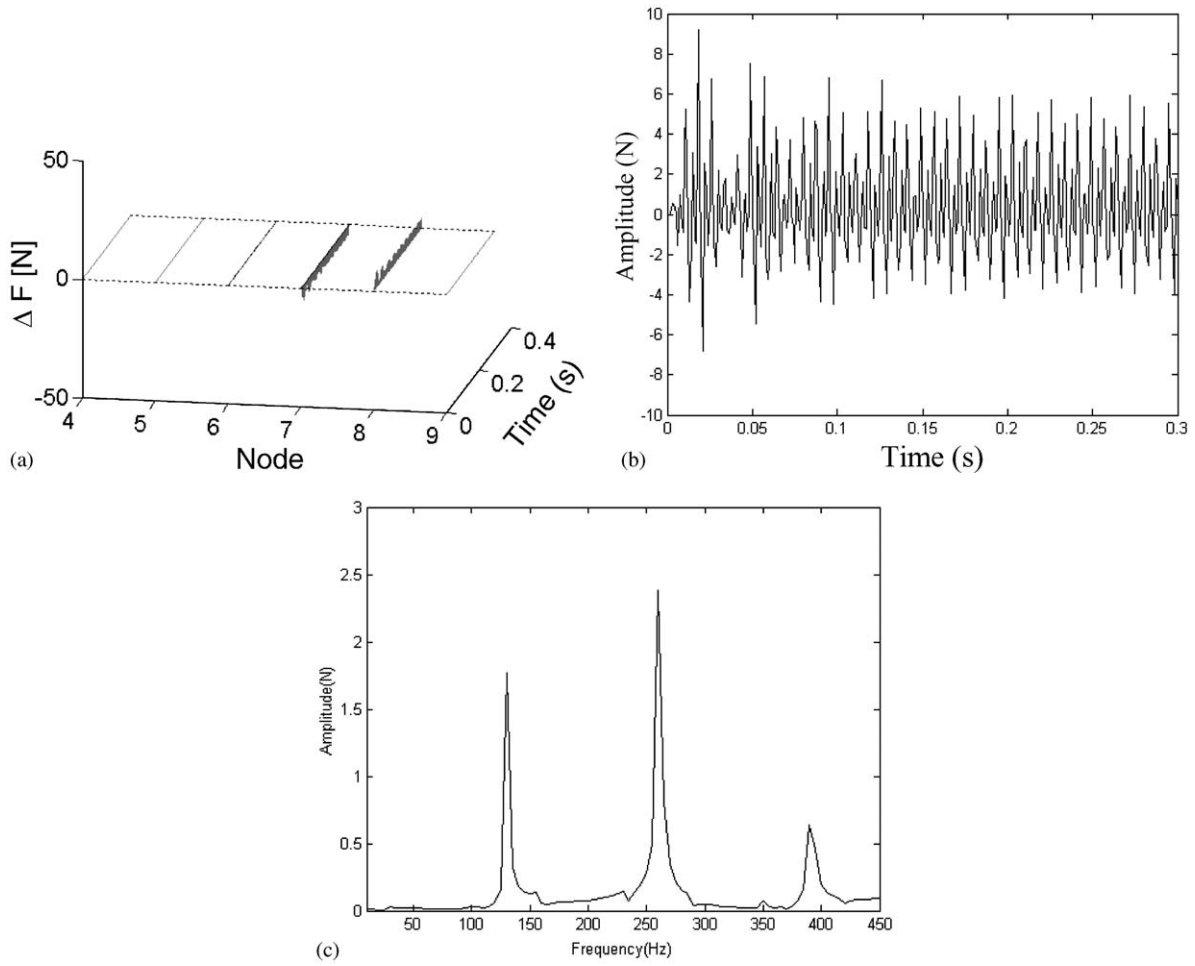

Fig. 11. Identification of crack of depth 2 mm in element 7 (8 DOF) at rotor speed of 130 Hz: (a) estimated equivalent loads, (b) time domain, (c) FFT.

Acknowledgements

The author would like to thank the Alexander von Humboldt Foundation for financial support to carry out this research. Also, he would like to thank, Prof. R. Markert and his work group for providing, support, discussion and facilities.

References

[1] J. Wauer, Dynamics of cracked rotors: literature survey, *Applied Mechanics Reviews* 43 (1990) 13–17.
[2] R. Gasch, A survey of the dynamic behaviour of a simple rotating shaft with a transverse crack, *Journal of Sound and Vibration* 160 (1993) 313–332.

[3] A.D. Dimarogonas, Vibration of cracked structures: a state of the art review, *Engineering Fracture Mechanics* 55 (1996) 831–857.
[4] L. Hamidi, J.B. Piand, H. Pastorel, W.M. Mansour, M. Massoud, Modal parameters for cracked rotors—models and comparisons, *Journal of Sound and Vibrations* 175 (1994) 265–278.
[5] S. Seibold, K. Weinert, A time domain method for the localization of cracks in rotors, *Journal of Sound and Vibration* 195 (1) (1996) 57–73.
[6] H. Bach, R. Markert, Determination of the fault position in rotors for the example of a transverse crack, in: Fu-Kuo Chang (Ed.), *Structural Health Monitoring*, Technomic Publ., Lancaster/Basel, 1997, pp. 325–335.
[7] R. Platz, R. Markert, M. Seidler, Validation of online diagnostics of malfunctions in rotor systems, *Proceedings of the Seventh International Conference on Vibrations in Rotating Machinery*, IMech, UK, 2000, pp. 581–590.
[8] R. Markert, R. Platz, M. Seidler, Model based fault identification in rotor systems by least squares fitting, ISROMAC-8, Honolulu, Hawaii, March 2000.
[9] S. Edwards, A.W. Lees, M.I. Friswell, Estimating rotor unbalance from a single run-down, *Proceedings of the Seventh International Conference on Vibrations in Rotating Machinery*, IMech, UK, 2000, pp. 323–334.
[10] N. Bachschmid, P. Pennacchi, Model based malfunction identification from bearing measurements, *Proceedings of the Seventh International Conference on Vibrations in Rotating Machinery*, IMech, UK, 2000, pp. 571–580.
[11] N. Bachschmid, R. Dellupi, Model-based diagnosis of rotor systems in power plants—a research funded by the European community, *Proceedings of the Sixth International Conference on Vibrations in Rotating Machinery*, IMech, Oxford, UK, 1996, pp. 50–55.
[12] I. Mayes, J.E.T. Penny, Model-based diagnostics of faults rotating machines, *Proceedings of the 12th International Congress on Condition Monitoring and Diagnostic Engineering Management*, Sunderland, UK, 1998, pp. 431–440.
[13] H.D. Nelson, J.M. McVaugh, Dynamics of rotor-bearing systems using finite elements, *American Society of Mechanical Engineers Journal of Engineering for Industry* 98 (1976) 593–600.
[14] C.A. Papadopoulos, A.D. Dimarogonas, Coupled longitudinal and bending vibrations of a rotating shaft with an open crack, *Journal of Sound and Vibration* 117 (1987) 81–93.
[15] A.S. Sekhar, B.S. Prabhu, Transient analysis of a cracked rotor passing through the critical speed, *Journal of Sound and Vibration* 173 (1994) 415–421.